Journal of Applied Science and Environmental Studies
JASES
http://revues.imist.ma/index.php?journal=jases

PERFORMANCE ANALYSIS OF A STAND-ALONE PHOTOVOLTAIC SYSTEM IN THE SAHARAN ENVIRONMENT

O. KEBOUR[1], A. HADJ ARAB[2].

[1]*Université de Saad Dahlab, Route de Soumaa, BP 270 BLIDA OuledYaich 09200, Algérie. Tél : +213661523799, Email :kebour.omar@yahoo.fr*

[2] *Centre de Développement des Energies Renouvelables, CDER, BP 62 Route de l'Observatoire, Bouzaréah 16340, Algiers, Algerie. Tél : +213540016638. Email : a.hadjarab@cder.dz*

Received 28 Nov 2020; Revised 20 Jan2021, Accepted 21 Jan 2021

ABSTRACT

Electrification of rural population has been always a strategic decision for the counties with high potential in terms of solar energy. However, different renewable and sustainable energy technologies can be adopted for electrification including photovoltaic system, diesel or hybrid system (photovoltaic and diesel). However, the choice between these options is exclusively dependent on many factors including the reliability and the cost associated with these technologies.

This study aims to examine the reliability of the electrification of rural areas using a standalone photovoltaic (PV) system in a Sahara environment (Algerian desert). In order to assess the electrical performance of the photovoltaic system, an experiment is set up in the village of Fadnoun, which is located in 2100 km south of Algiers (Algerian capital). The experiment is carried out for one year and the reliability of the system together with the way in which this electrification influence the energy consumption the villagers are assessed. It should be noted that this is the first experimental study of this kind that has been carried out in Algeria.

In addition, a technical-economic analysis was conducted by taking into account many parameters including cont, nominal power, solar radiation, and low voltage length. The outcomes of this study can be used as a benchmark to assess the performance of renewable energy technologies in other rural areas and make an informed decision about the most appropriate technology for electrification in rural areas.

1. Introduction

Sahara regions receivea greater amountof energy that makes them as favorite locationsto set up thephotovoltaicsystems. In order toensure continuity ofservice, for a number of Algerian Sahara villages, two principal and independentenergy supply solutions can be practically considered that include diesel generators andphotovoltaic systems.

The main research question is to identify the most economical solution among diesel and PV for any given site.

Itshould also be pointed out that this method of segmentation is used within the Algerian National Electrical Grid Company "Sonelgaz Holding" as a dashboard to identify areas where the turnover is high, and where industrialcustomers sectors are segmentedin relation to their sector of activity and the power available (PMD) [1].

One of the early studies in this field was by[2] in order to develop a redistribution mapping of Algerian territory or zoning, it is based on hygrothermal considerations. In addition were reported for just one representative day.

In another study, [3] evaluated solar irradiation level in Algeria; four climatic zones were identified for a different clarity index based on energy factors such as solar irradiation at ground level and determination of the probability of loss, for a period of twelve months. The results of this study have shown that the effect of the micro climate is too great on the determination of climatic zones.

In an attempt to improve the accuracy of the numerical models in estimation of solar radiation, [4] has developed physical and empirical models to estimate the hourly, daily and monthly solar radiation from multiple sources. The developed models are applied and tested for different climatic regions in Algeria and consequently a zoning map of solar radiation is proposed.

In another study, a numerical model for economic profitability of a photovoltaic pumping plant was developed by [5]. The outcomes of this numerical modelling demonstrated the importance of economic competitiveness in the selection of diesel engine system compare to photovoltaic in the field of water pumping. The adopted method was based on the calculation of the overall cost of the cubic meter of water pumped based on expressed needs (height, maximum speed, and irradiation).

In addition, a number of studies on hybrid renewable energy systems have been conducted in different parts of the world where hybrid photovoltaic systems with energy storage have been modeled. The outcomes of these studies showed that hybrid systems have enormous technical and economic benefits [6].

In another study[7] conducted a technical-economic analysis to assess the feasibility of the hybrid photovoltaic-diesel engine system in Ghana. Results of this study highlighted that technical, economic and environmental feasibility of the system for a context with a medium irradiation level and relatively low fuel cost.

[8]used the same approach with complete environmental monitoring. The results of experiment were based on an analytic model together with the economic and the environmental models to compute the LCoE. A parametric tool, implementing such models according to the introduced energy flow control algorithm, varying the PV plant rated power. Taking into account the effect of the low-voltage grid (L_{BT}), they would have varied the low-voltage length of the network

[9, 10] conducted a technical, conceptual and economic analysis for a complete hybrid system that includes photovoltaic modules, micro-turbines and batteries (as an emergency power source) for a remote community in the Palestinian territories. However, this work was limited to only one case

In an attempt to improve the accuracy of the numerical models in estimation of the energy performance and the competitiveness, [11] have studied in the case of Tamil Nadu (India) for

different climatic zones on the basis of the current net cost. The results of this study have shown that government subsidies are essential to attract interest in renewable energy because they require capital, where people are poor and therefore unable to bear.

One of the most recent studies in this same field has been carried out by [12]. They investigated the energy performance of naturally ventilated PV façade systems using both experiment and simulation. A numerical model based on TRaNsientSYstem Simulation (TRNSYS) package was developed to assess the thermal and energy performance of the system. However, the economic aspect has not been addressed.

From the literature review, it is evident that there have been a few studies concerning the electrification of villages using an autonomous photovoltaic system were carried out in Algeria, unlike photovoltaic pumping works [13, 14]. In addition, the developed numerical models to simulate the different irradiation and performance of the system PV were mainly validated using experimental data collected over a limited period, which could not represent the varying operative conditions of the system.

The aim of this research is to study the reliability of the electrification of rural areas using a standalone photovoltaic (PV) system in a Sahara environment (Algerian desert), in order to assess the performance of the PV system in such an environment for a whole year, the reliability and the villagers lifestyle impact on the energy consumption as well was checked. In addition, a technical-economic analysis was conducted by taking into account many parameters including cost, nominal power, and solar radiation and Low Voltage length. The outcomes of this study can be used as a benchmark to assess the performance of renewable energy technologies in other rural areas and make an informed decision about the most appropriate technology for electrification.

2. Experimantal details

The exploitation of solar energy photovoltaic (PV) systems requires accurate knowledge of the distribution of solar radiation, which depends on several geographical, meteorological and astronomical parameters, where the system needs to be installed.

This study is designed in two main parts. In the first part, an experiment to assess the performance of a system PV. The details of experiments are provided in Section 4.

In the second step, is about comparison between the two solutions of electrification, Diesel and photovoltaic under real conditions, using a mathematical approach developed for this purpose.

2.1 Models description

The objective is the validation and comparison of the calculated and measured results of the model used for different illumination and temperature conditions.

2.1.1 Solar irradiation

Simulation methods which are currently used depend on the amount of daily solar irradiation. For this experiment, models based on mathematical equation were used in order to calculate different components of solar radiation[15]. The outcomes of this model were evaluated using measured data of Tamanrasset site.

2.1.1.1. Direct and diffuse horizontal irradiance component estimation:

The determination ofdirectand diffuse componentsofthe horizontalirradianceis required for the irradiance calculation on an inclined surface.

The daily diffuse horizontal irradiance $D_d(0)$ is obtainedfromthe correlationbetweenthe fractiondiffuse$K_d$and the atmosphere clarity indexK_t,the diffuse fractionisdefined asK_d[16, 17]:

$$K_d = \frac{D_d(0)}{G_d(0)} \qquad \textbf{(1)}$$

And the atmosphere clarity index K_t as:

$$K_t = \frac{G_d(0)}{B_d(0)} \qquad \textbf{(2)}$$

The daily horizontal direct irradiance $B_d(0)$ is given by [18]:

$$B_d(0) = G_d(0) - D_d(0) \qquad \textbf{(3)}$$

2.1.1.2. Frutos Model

The correlation between the individual daily horizontal irradiance $G_d(0)$ and its diffuse component $D_d(0)$ is [13, 19]:

For $K_t < 0.166$ interval

$$K_d = 0.92 \qquad \textbf{(4)}$$

For $0.166 \leq K_t \leq 0.8$ interval

$$K_d = 0.77 + 1.93K_t - 6.86K_t^2 + 4.27K_t^3 \qquad \textbf{(5)}$$

For $K_t > 0.8$ interval:

$$K_d = 0.109 \qquad \textbf{(6)}$$

2.1.1.3. Estimation errors

The comparison, between calculated and measured data, by using Frutos model is done by using a statistical indicator called root mean squared error (RMSE) defined as:

$$RMSE = \left[\frac{\sum_{i=0}^{N}(C_i - M_i)^2}{\sum_{i=0}^{N} M_i^2}\right]^{0.5} \times 100 \qquad \textbf{(7)}$$

Where $C_i$is the i^{th}calculated value, $M_i$$i^{th}$ measured value and N is the number of point. The root mean squared error (RMSE) is a measure of the variation of measured value closed to the calculated value.

2.1.1.4. Irradiance on tilted surface

For the purposesof this calculation, it is considered that one-hour radiationnumericallycoincides with theaverage irradianceduring thishour.

The global irradiance on a tiltedsurfaceinthe earth's surfaceG (β) can be calculatedas the sumof thedirect radiationB (β),diffuse radiation D (β) and the reflected radiation R (β):

$$G(\beta) = B(\beta) + D(\beta) + R(\beta) \qquad \textbf{(8)}$$

A new application of irradiance estimate for photovoltaic (PV) applications has been studied by [20].

2.1.1.5. Direct radiation

Direct component of irradiance beam $B_h(\beta)$ can be obtained by using the incident angle θ_s and zenith sun θ_{zs}:

$$B(\beta) = \frac{B_h(0)\cos\theta_s}{\cos\theta_{zs}} \quad \textbf{(9)}$$

2.1.1.6. Diffuse radiation, Hay and McKay Model

The Hay model used [21] consider two area of the sky as diffuse irradiance sources: one partcharacterized byisotropicemission(consider sky diffuse irradianceas uniformly distributed) and the other (thecircumsolar), comesdirectly.

$$D(\beta) = D_h(0)\left[\frac{G_h(0)-D_h(0)}{B_{oh}(0)}\frac{cos\theta_s}{cos\theta_{zs}} + \frac{(1+cos\beta)}{2}\left(1-\frac{G_h(0)-D_h(0)}{B_{oh}(0)}\right)\right] \textbf{(10)}$$

$$B_{oh}(0) = B_o\left[1+0.033cos\left(\frac{360d_n}{365}\right)\right]cos\theta_{zs} \textbf{(11)}$$

2.1.1.7. Reflected radiation

Reflected radiation or albedo on top tilted surface is given by [18]:

$$R(\beta) = \frac{1}{2}\rho G_h(0)(1-cos\beta) \quad \textbf{(12)}$$

Where ρ is ground reflectivity and in the absence of specific information, we use $\rho = 0.2$.
The RMSE calculation result for the site of Tamanrasset titled at 30° (latitude angle) is 15.8%.

2.1.2. Photovoltaic generator model

The aim of this model is to represent the generator current versus voltage, temperature and received illumination.
PV generator (Fig. 1) consists on an assembly of photovoltaic modules. Each module is made of an assembly of photovoltaic cells connected in series to make strings that are connected in parallel in order to obtain the right voltage and current[22].

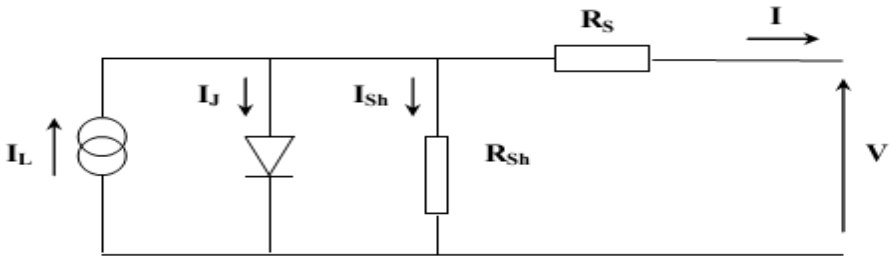

Fig. 1. Synoptic schema of PV generator.

I is the current and V the voltage of at the circuit terminals.
Kirchhoff's law allowed us to write this equation:

$$\boldsymbol{I_L = I_J + I_{sh} + I} \quad \textbf{(13)}$$

The current flowinginthe shunt resistorisgiven by the expression:

$$\boldsymbol{I_{sh} = \frac{V+IR_s}{R_{sh}}} \quad \textbf{(14)}$$

Junction current is given by:

$$\boldsymbol{I_J = I_0\left[exp\left(\frac{e(V+IR_s)}{mKT}\right) - 1\right]} \quad \textbf{(15)}$$

Putting I_J and I_L expressions, we obtain the relation between the current (I) and the voltage (V):

$$\boldsymbol{I = I_L - I_0\left[exp\frac{V+IR_s}{mV_t}\right] - \frac{V+IR_s}{R_{sh}}} \quad \textbf{(16)}$$

with

$$V_t = \frac{k.T}{e} \quad \textbf{(17)}$$

Where $\boldsymbol{I_L}$ is the yield current due to charge carriers that occur due to radiation.I_0 is the saturation current, R***s***is series resistance, m is the ideality factor, R***sh*** is the parallel resistance, K is the Boltzman's constant, T is the cells absolute temperature and e is the electron charge.
The equationis implicit, so to resolve it, it requires iterative methods. There are different models to obtain $\boldsymbol{I_L}$,$\boldsymbol{I_0}$, m, $\boldsymbol{R_s}$ and $\boldsymbol{R_{sh}}$ of 16 equation.
In this work, the analytical model was chosen[23].
For a given irradiance and temperature, the five parameters ($\boldsymbol{I_L}$,$\boldsymbol{I_0}$, m, $\boldsymbol{R_s}$ and $\boldsymbol{R_{sh}}$) can be determined from following data that are open circuit voltage (V_{OC}), short circuit current (I_{SC}), maximum current (Im) and maximum voltage (Vm) and the slope around (Voc) and I_{SC}[24].

$$\left(\frac{dV}{dI}\right)_{V=V_{oc}} = -R_{so} \quad \textbf{(18)}$$

$$\left(\frac{dV}{dI}\right)_{I=I_{sc}} = -R_{sho} \quad \textbf{(19)}$$

The obtained equations are [25]:

$$m = \frac{V_m + I_m R_{so} - V_{oc}}{V_t\left[\ln\left(I_{sc} - \frac{V_m}{R_{sh}} - I_m\right) - \ln\left(I_{sc} - \frac{V_{oc}}{R_{sh}}\right) + \left(\frac{I_m}{I_{sc} - \frac{V_{oc}}{R_{sho}}}\right)\right]} \quad \textbf{(20)}$$

$$I_0 = \left(I_{sc} - \frac{V_{oc}}{R_{sh}}\right) \exp\left(-\frac{V_{oc}}{mV_t}\right) \quad \textbf{(21)}$$

$$R_s = \left(R_{so} - \frac{mV_t}{I_0}\right) \exp\left(-\frac{V_{oc}}{mV_t}\right) \quad \textbf{(22)}$$

$$I_L = I_{sc}\left(1 + \frac{R_s}{R_{sh}}\right) + I_0\left(exp\frac{I_{sc}R_s}{mV_t} - 1\right) \quad \textbf{(23)}$$

$$R_{sh} = R_{sho} \quad \textbf{(24)}$$

Once we have characterized the photovoltaic module, the generator is modeled as NS modules combination in series and NP modules in parallel, assuming that they are identical.

2.1.2.1. Error computing

The standard error is defined by [26]:

$$ES = \left[\frac{\sum(I_{cal} - I_{exp})^2}{N}\right]^{0.5} \quad \textbf{(25)}$$

Where $I_{cal}$and I_{exp} are respectively the calculated and measured currents and N the number of measuring points (Fig. 2).

The error:

$$E_x = \frac{X_{cal} - X_{exp}}{X_{exp}} \times 100 \quad \textbf{(26)}$$

Being X :I_{sc} , V_{oc} and P_m.

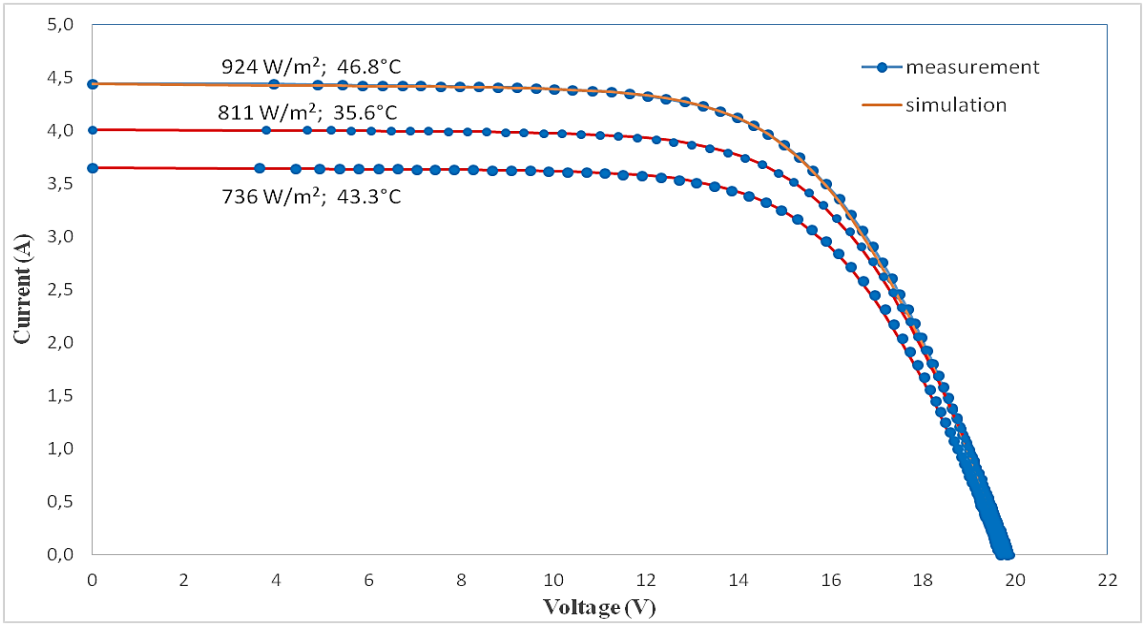

Fig. 2. Experimental and calculated I-V curve applying analytical model to PV module (PhotoWatt) at different irradiance and different temperatures.

Table 1 gives the obtained errors measures between the measured values and the calculated ones using the five parameters model.

Table 1

Application sample (PhotoWatt).

Irradiance (W/m^2)	924	736	811
Temperature (°C)	46.8	43.3	35.6
EI (A)	0.0217	0.0193	0.0168
Ex(%)	1.0625	-3.9015	-1.4249

For the analyzed examplesapplied to mono crystalline siliconphotovoltaic modulethat feeds Fadnoun village with 736 W/m^2,811 W/m^2 and924W/m^2 irradiance and temperature ranging between 35.6°C,43.3°Cand 46.8 °C, theerrors are small. The modelfitswith great accuracy theI-V characteristicandconvergesinall studied cases. However, itrequiresgood measuresin adjacent areaswith I_{SC}, Voc, ImandVmand measuringslopesinI_{SC} and in Voc.

2.2. Electricity production cost calculating

To assess the competitiveness of an electrification solution it is necessary to know the cost of producing electricity [27].

The calculation of the levelized cost per kWh compares technologies whose life is different (40 for networks; 20 years for photovoltaic; 15 for diesel) [28].

The cost function consists of fixed and variable expenses. Fixed expenses represent initial investment (generator, battery, installation costs: converters, medium and low voltage power lines) while variable costs consist primarily of fuel cost.

The various rural electrification solutions adopted are classified into three groups [29]:

* Individual systems where semi collective; PV Array;

* Low voltage local mini-grid electrification through micro diesel plant.

* By connecting an existing network (medium and low voltage).

According to equation (27), the average discounted cost of electricity is definedas the sum of the annual expenditure to date on the sum of the annual electrical production.

$$P = \frac{\sum_{i=1}^{n} A_i . I_i + D_i}{E} \quad \textbf{(27)}$$

The annuity factor for equipment is defined by

$$Ai = \frac{1}{\sum_{n=1}^{n1} \frac{1}{(1+a)^n}} = \frac{a.(1+a)^{Ni}}{(1+a)^{Ni} - 1} \quad \textbf{(28)}$$

with

index « i » : means generator; battery ; line « L_{BT}» ; or transformer.

2.2.1. Selecting the optimal solution

Considering various projects that provide the same services, the preferred option is the one that would lead to the minimum economic unit return cost.

2.2.1.1. Solar photovoltaic energy solution

The formula which gives us the equivalent cost of electricity in kWh as follows[28]

$$\text{PV cost} = \frac{(A_{PV}+H_{PV})xP_{PV}xC_{PV}+(A_{bat}+H_{bat})xP_{bat}xC_{bat}}{Ec} \quad \textbf{(29)}$$

After introduction of the various parameters and computing, equation (29) becomes:

$$PV\ cost\ =\ 57.74\ +\ \frac{480}{\mathrm{EG}(\beta,\mathrm{ti})} \quad \textbf{(30)}$$

2.2.1.2. Diesel electrical solution

The average purchase cost of diesel generator includes the capital cost of the diesel generator, the cost of the L_{BT} (low voltage line) connection, operating costs and the cost of fuel needed to meet electricity demand.

Operating costs are estimated as a percentage of the investment cost.

$$\text{D cost} = \frac{(A_D+H_D)xI_D+(A_{BT}+H_{BT})xI_{BT}+C_{fuel}}{Ec} \textbf{(31)}$$

D cost Average discounted diesel solution cost (USD/kWh).

After integration of all parameters for calculating the cost of diesel kWh depending on the low voltage line and the annual consumption of electrical energy (L_{BT}, Ec).

Equation (31) becomes. $D\ cost = 117.63 + 68058x\frac{L_{BT}}{Ec}$ **(32)**

3. Description of the mini photovoltaic plant and data (Case study)

Our case study includes two parts, the first deals with a study and analysis of the photovoltaic system performance, based on site measurements. The second part is about comparison between the two electrification solutions, Diesel and photovoltaic in real conditions.

The village description is given below.

3.1. Village description

Fadnoun is a small size village located in the south-east of Algeria, 2100 km far from the capital Algiers, 300 km from the district of Illizi and 305 km from Djanet. From the northFadnoun is limited by the county of Bordj El Houes, Lybia from east and Tamanrasset from West (Table 2).

Table 2

Geographical locationand meteorologicaldataof the villagefor 2013 [30].

Latitude (°)	Longitude (°)	Altitude (m)
22.78 N	05.52 E	1377

Fadnoun is a village oftraditionalhouses surrounded bysomezeribates(pluralofZeriba), where Terguis population (originally nomads) live. They are about 60Bedouins(Population censusin 2011) settledin this village, after the advent of the southern development special programfund in 2001.

The zeriba is a house made of a single piece of rounded shape, whose appearance is reminiscent of an African village hut.

There are no income-generating activities except for a small portion of the population which is engaged in breeding goats and camels.

Fadnoun village is classified [30];

- National Park in 1972.
- Mixed cultural and natural site of Humanity by UNESCO in 1982.

•Biosphere Reserve of Program ' Man and the Biosphere" by UNESCO in 1986.

Because of the fact that the village is far from the national grid power on one hand, and the major constraint represented by its location (Heritage protected by UNESCO) on the other hand, the stand-alone PV system offers a very cost-effective solution;
This stand-alone PV system can be used to meet people energy needs to light houses, use a refrigerator, watch TV and benefit of low power consumption applications goods for the first time in their life.
Currently, the village of Fadnoun (Fig. 3) consists of:

- Twenty (20) houses with two rooms (F2) consisting of solid construction, connected to electricity.
- One (01) three rooms (F3) accommodation consisting of solid construction for the three primary school teachers.
- One (01) primary school with one classroom for 45 pupils.
- One (01) two rooms (F2) prefabricated infirmary, bathroom included.
- A place of worship consisting of a prefabricated (01) room.
- A grocery supplied with individual PV kit.
- A six (06) meter height water tower operating with a generator and feed the village by gravity.
- Two telecommunication antennas powered by two diesel generators.

Fig. 3. Overview of thevillage ofFadnounwith other equipment

Many experiments and measurements took place for a period of one year in real operating conditions in order to check, observe the installe PV system and improve its profitability and efficiency. Among those actions, the change of the electricity demand of the village by replacing all incandescent lamps by low consumption on the one hand, and secondly, interventions due to electrical faults. Also, the cleaning of the photovoltaic modules enabled to ensure continuity of service and good quality service [31, 32, 33, 34].

3.2 Description of data acquisition system

The data acquisition device consists of:

- Current and voltage equipment.
- Thermometer (placed on PV module).

- Clamp meter.
- Calibrated solarimeter (mV/cm^2) placed on solar module front.
- Three phase electric-meter energy counter with indirect connection SAGEM CX2500-4CLK CT.

Communication with the SAGEM counter is in local mode via an optical probe, directly connected to the computer.
The use of the load curves data (covering a period of one year with measurement every 30 minutes), on one hand and energy balance of the town, on another hand, allowed a clear vision about the behavior of power consumption of both villagers and photovoltaic system.
The analysis of the energy consumption of the village should be conducted as close to the actual consumption process [35].

3.3Description of the various parts of the photovoltaic system

To provide the required electrical demand a photovoltaic system consists of a generator, generally associated with one or more of the following [36]:
Electronic management(shapingof the current,energy transfer)- Storage system- AC/DC Inverter-Low voltage direct current load or alternating current load (Fig.4).
Thebelowshows the arrangementof thevarious componentsin a stand-alone photovoltaicinstallation.

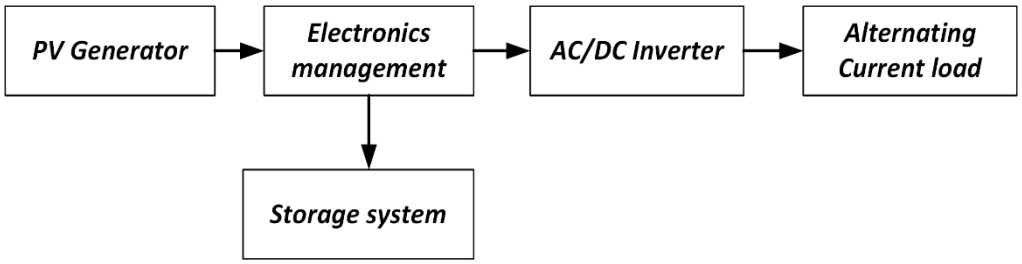

Fig. 4. Block diagramof astand-alone photovoltaic system.

The photovoltaic PV system that feeds the village consists of three independent subsystems:
two 4.5 kWp and one 1.5 kWp. A technical room consisting of solid construction used to support the solar modules metallic structure.
The electrical connection of the village is made as follows

Subsystem 3 and 2: 2x10 homes electrification.
Subsystem 1: small administrative building electrification.

3.3.1. Photovoltaic system design

The performance prediction and sizing of the autonomous photovoltaic system requires the use of a daily solar radiation with its unpredictable variations[37], and a precise analysis of electrical needs and different factors which affect their yields: meteorological data and installation surroundings [38].

3.3.1.1. Computing of the energy output of the photovoltaicsystem
Subsystem N°2

Calculation of the energy produced by the PV subsystem 2 E_{pg}

$$E_{pg} = \left(E_{cj}/(\eta_s \times \eta_r \times \eta_c)\right) \quad \textbf{(33)}$$

$$E_{pg} \leq N_m \times E_{pm} \textbf{(34)}$$

3.3.1.2. Computing of the energy output of photovoltaic modules E_{pm}
Following the equation below we have:

$$E_{pm} = E_{RI\ min} \times \eta_m \times A_m \times F_r \quad \textbf{(35)}$$

$$N_m = 45 \text{ modules}$$

Association of modules
Once the number of modules known, the equivalent necessary configuration of series-parallel connected modules is determined.
Series connection

$$V_m \times N_{ms} \geq V_t$$

$$\text{that gives} \quad N_{ms} \geq 4 \textbf{(36)}$$

Parallel connection

$$N_{bp} = N_m/N_{ms} \text{ Then } N_{bp} = \frac{45}{4} = 12 \quad \textbf{(37)}$$

In shortthePV arrayconsists of 12 strings where in each one 04modules are connected in series.

Subsystem N°3
By adoptingthe same calculation, 42 modulesare used in ten (10) strings. In each string, four (04) modules are connected in series.

Subsystem N°1
By usingthe same method, an arrayis made of16 PV modules: four (04) strings made of four (04) modules connected in series.
It is noticed that the over sizingby 14% of the given PV system, is due to the fact the village isexpandable, and to the complexityof suchinvestment. These facts lead to the assumption that local authorities made this formula knowingly.

3.3.2. Storage system design (battery bank)
The storage capacity according to the necessary autonomy is given by the following relationship:

$$C_s = \left(N_j \times E_{cj}\right)/(P_d \times V_s \times \eta_s \times \eta_r \times \eta_c) \quad \textbf{(38)}$$

The nominal storage system voltage V_S is equal to the installation functioning voltage. The number of the system day's autonomy $N_j$is fixed to 04 days.

Subsystem N°2 and N°3

After computing, it is found that: $C_S = 1420\ Ah$

$$C_{10} = \frac{Cs}{Fcs} \textbf{(39)}$$

$F_{CS} = 1.25 \text{for} 1 \leq N_J \leq 4$

Thus $C_{10} = 1136\ Ah.$

Subsystem N°1

For subsystem 1, it is found that: $C_{10} = 420\ Ah$

Connection of batteries in « Series-parallel»:

By using 2 Volt batteries, so to get a voltage of 48 Volts, 24 batteries are connected in series (Fig. 5).

Fig. 5. Batteries bank.

The over sizing of the storage systems is 40%, 40% and 70% for subsystems 3, 2 and 1 respectively.

This over sizing will limit temperature and provide the necessary energy for system operation and control.

3.4Procedures andsurvey results

For a whole week, the system was continuouslychecked andinspected in order to check thestateoftheoperationbefore startingmeasurements.

This is toremove all theproblems that coulddisruptor distortthe sequence ofmeasures(developmentofallfullinstallation).

Finally,after beingassured thatthe systemoperates well,thePV systemperformanceassessmentprocess beginswith monitoring over a periodof one year.

In order to obtain the maximum information on the operation of the PV system during this period, a monitoring of the evolution of the various parameters mentioned above 24 hours a day with a step of 30 minutes through the SAGEM CX 2000-4 meter.

Also,to fullyconsolidatedata acquisitionsystem, Touaregvillagerswere trainedto vary all parameters andfeatureson the SAGEMcounterfor the durationof the measurements campaign.

The experimentwas focused oneach photovoltaic system component, upstream and downstream, namely solarradiation, PV generator,the storage systemand the converter.The results obtainedareanalyzed and discussed below:

1. Results and discussion

3.1. Analysis of site solar irradiance

The analysisof this parameteris very importantbecause of its plays a key role in thedesign of aPV systems, in fact, the knowledge of itsevolution over time, givesan exact ideaabout the solarpotential of Illizi region. To do thisfirst it is necessary tounderstand the level of irradiation of the Fig. 6.

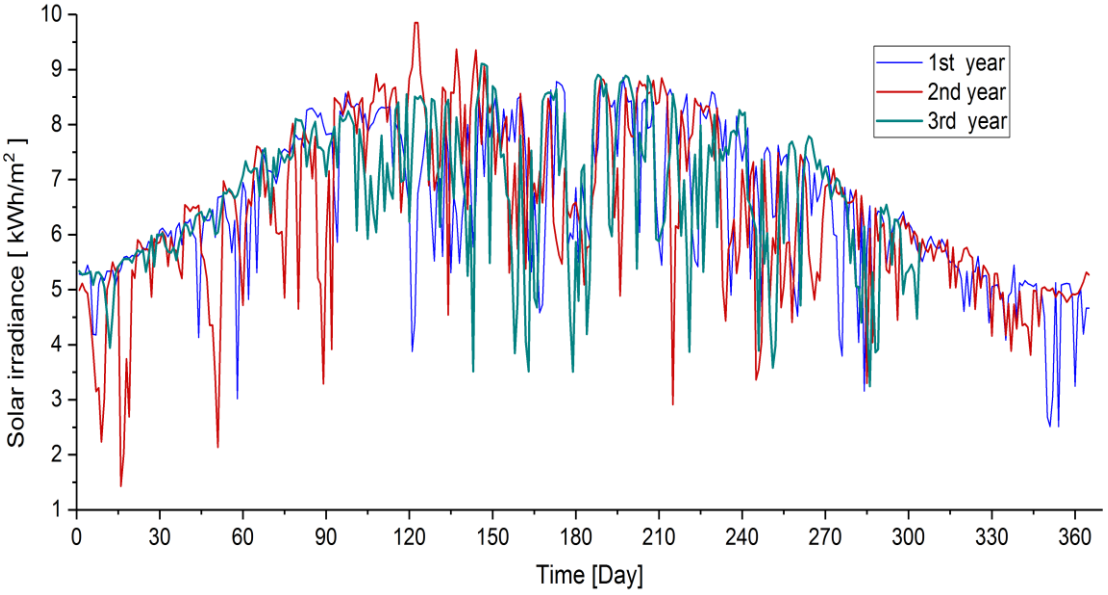

Fig. 6. Solar irradiance evolution during the three years.

Toanalyze the evolutionof the prevails irradiance (Fig.7), the data is splitinto four partsof three months. This is done toanalyze eachquarterapartand deducethe overall behaviorof the annualirradiation [39].

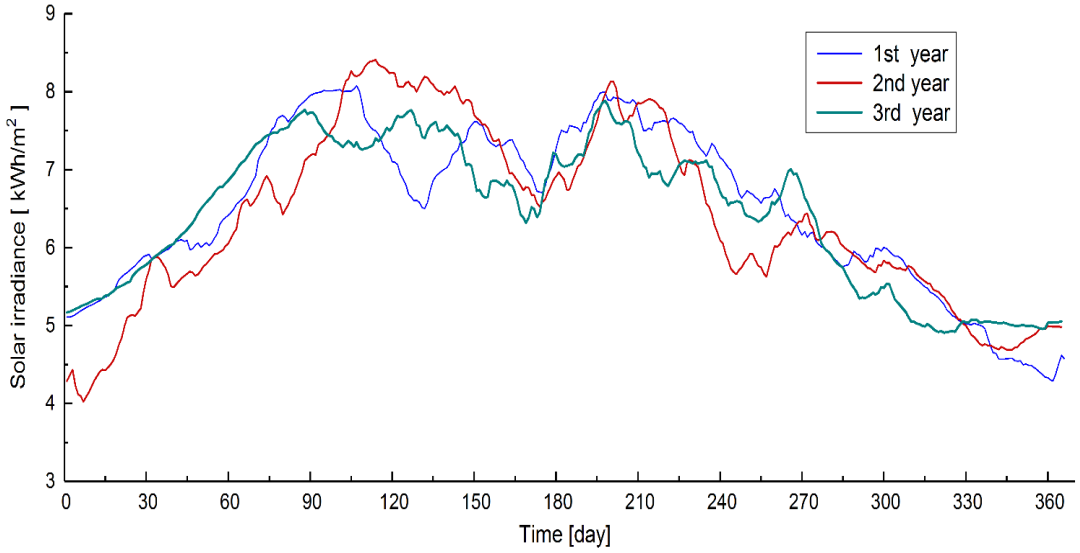

Fig. 7. Solar irradiance evolution during the three years after smoothing.

The curve of the third year is chosen as the basic element ofallcalculations.To see the evolution of solarirradiation better,two days are chosen fromtwo representativemonthsof this same curve, which are June and July.

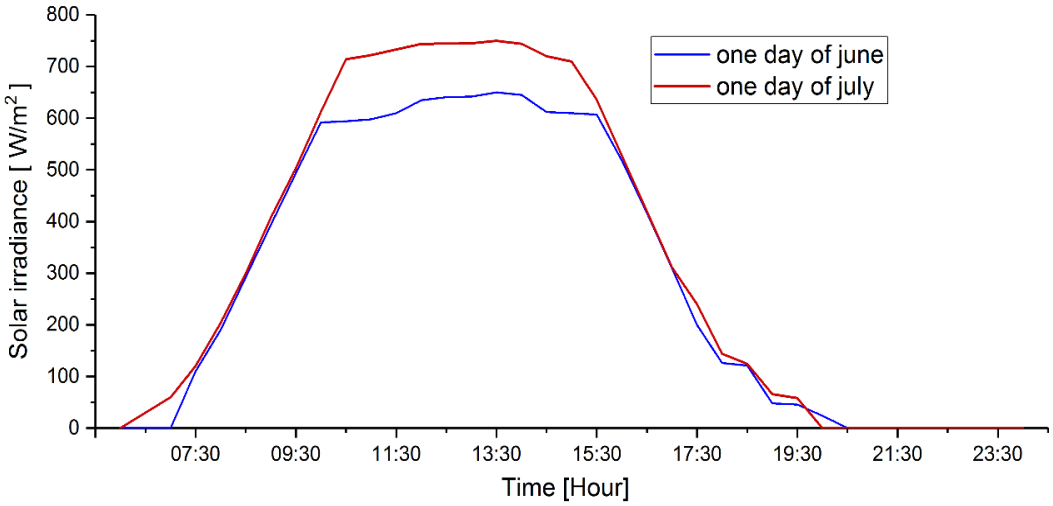

Fig. 8. Solar radiation evolution during the two days of June and July

With respect tothe radiation evolution, it is noticedfromthe given graphsin Fig. 8, that there is asimilarity betweenthe irradiancesreceivedduring the two days. In fact, a slight delayofirradiationappearsbecause of theovercast skyinthe early morningof the dayof June, and the peaksof radiationare observedatabout1 PM.

The average daily radiations values are given in the following Table 3:

Table 3
The average daily solar radiation receivedon photovoltaic modules surfaces.

Days	EG(β)j Wh/m^2/j	Emj W/m^2/j
The 15th of July	6528	593.05
The 15th of June	6435	558.95

3.2. Analysis of the photovoltaicsystem power generated

In this section, the behavior of thegeneratoris discussed, with the received radiationandambient temperature. (Fig. 9).

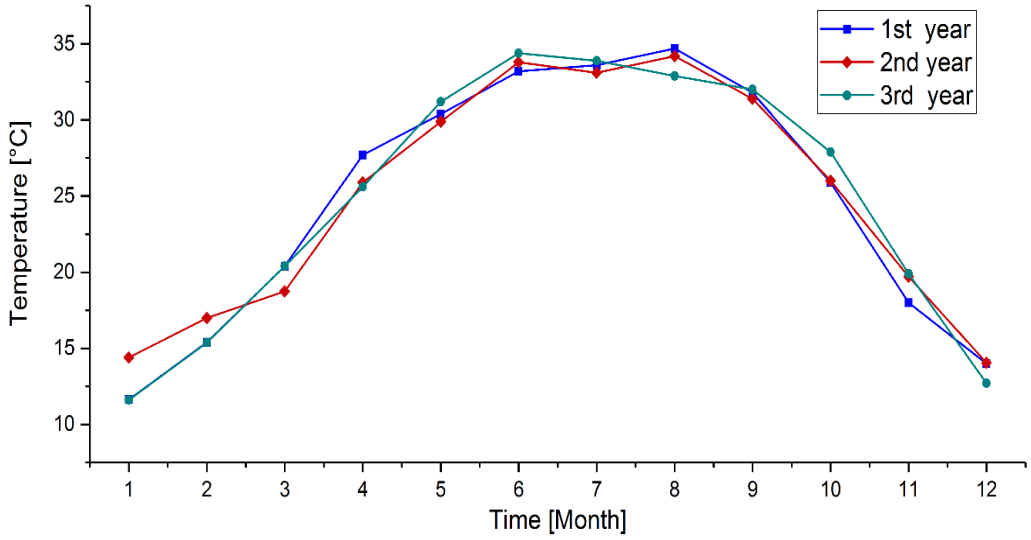

Fig. 9. Temperature evolution during the three years.

The figure 10.a and 10.b shows the evolution of the power generated by the panelsunder theaforementionedirradiation.An observationof thesecan detecttheexistingproportionality betweenthe irradiationand the powersprovided bythe panels; with a coefficient ofproportionalityis none other thanthe yieldsof the panels.Sothe totalpower generated bythegeneratoristhe sum of thesethree powerfractions, one of which represents a thirdof the other twoPG1=PG2/ 3=PG3/ 3 (Fig. 14.aand 14.b).

The evolution of thistotal powerwithirradiation asshown inthe graphsof Fig. 10.aand 10.b.appearsnormalfrom whathas just been said, except forthe periodof between1 PM. and 4:30 PM,where the curveregisters avisibledecline(Fig. 10.a). This decreaseresults inthatthe capacity of thebatteries, so thatbythetotal impedanceof the batteries.Whichacts on thecharacteristic(IV) of the generator by moving it tothe right (high voltages). Thisisjustified by thecurrentdecreases.

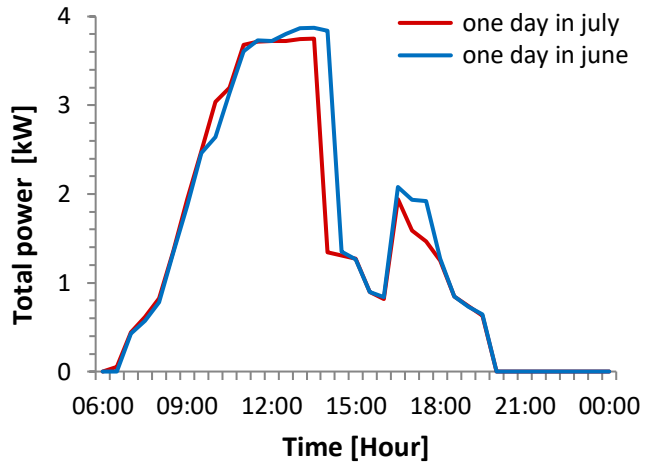

Fig. 10.a. PV system daily power generation in June and July.

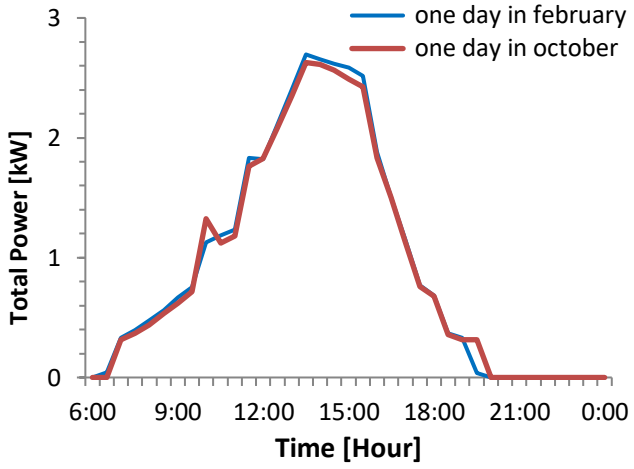

Fig. 10.b. PV system daily power generation in February and October.

Giventhe period of time ranging from 1 PM to 4:30 PM and the presence ofstrong sunlightwith high temperatures, this leads to think about the existence of twoother phenomenathat have led to this result.

The firstis due to theconversionof the limited power of the generator. In other words, increasing the illuminationfromcertainlimit valueis not reflectedby thecurrent suppliedby the generatorbutratherbysomeclippingofthe latter.Thislimitdepends on the qualityof the glass(glass transmittance), used driverthreshold andconditions of use.

The second phenomenonisaconsequence of the first. Indeed,the increase inilluminationbeyonda certain thresholdresults in asurpluson the percentage ofunconvertedlight energythat will bedissipatedasheatwithinthe modules.

This situation and the presence ofexcessive ambienttemperaturesaffect theevacuation processby natural convectionofthe heatdissipated insidethe modules, resulting in an increase of temperatureat the level of thesolar cells (Fig. 9).

Also, it isimportant to notethat the majority ofidentifiedcurvesshow the samepace,
characterizedby a declinein the sametime slotof the dayof the secondand thirdquarter of year (recorded on 80%of them)however,for the first andfourth quarterof the same yearthis singularityis not felton the set ofcurvesas wellasshown in Fig. 10.b.

It is important to note that the inverter power is much less than the PV power.

Also,thepower leveldifferencesrecordedby the curvesfor the twoperiods of the year, can reach 700 W.

Thesharp decrease in thepowerdevelopedby the generatorthat appears onthe graphs 10.acorresponds to solar panels disconnections (PG2 =PG3=0) by the tworegulatorssupplyinghomes.

The dailyenergydelivered by the generatorduring each day is given by Table 4:

Table 4
Dailyenergydelivered by the generator.

Days	**Edj [Wh]**
15th of July	40 358
15th of June	43 033

3.3. Generator conversion efficiency

In orderto achieve acorrect approachof actual performanceof the generator, the average yields are considered. These are snapshotsthroughout the day; except during theperiods whenthe threepanels are notall connected(performance during these momentsonly concerns theconnectedbranch).
The instantaneous efficiencies were calculated by the following equation:

$$\eta_c(ti) = PG\ (\ t_i)/(PG(\beta, t_i)) \textbf{(40)}$$

Power provided by irradiance on PV panels at t_i instant is given by:

$$PG(\beta, t_i)\ =\ G(\beta, t_i) \times A_G \textbf{(41)}$$

$$A_G\ = 50\ m^2$$

In Table 5 are representedthe average valuesof efficiencies of the PV generator.

Table 5
Average daily PV field efficiencies.

Days	ηc[%]
15th of July	10.13
15th of June	11.11

Thecurve shape of the function"efficiency vssolarcells temperature”obtained from theabove valuesηc= f(Tc) is plotted in Fig. 11.

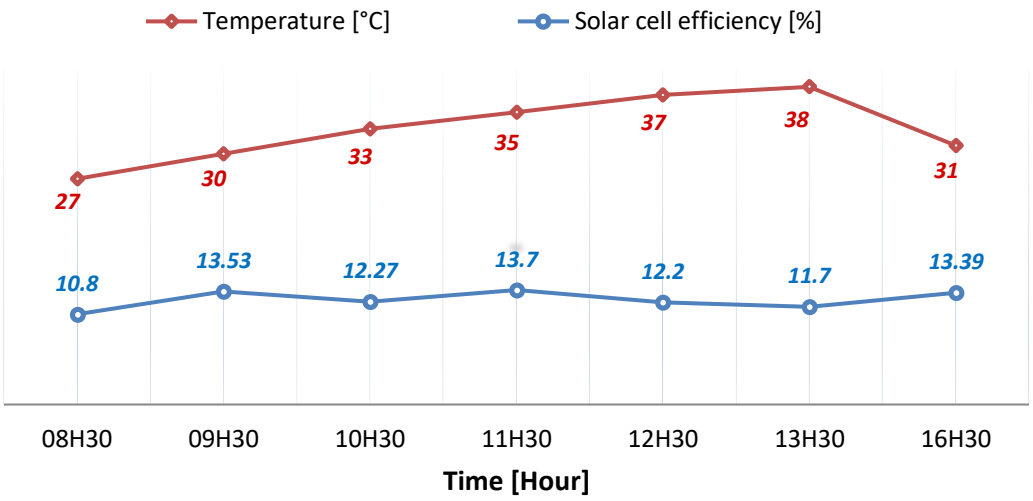

Fig. 11. Solar cell efficiency variation versus temperature.

3.4. Storage system

In this section the power charge and discharge is described, related data are given.

Charge and discharge time are illustrated in graphs given in Fig. 12.a and b for sunniest days (June and July).

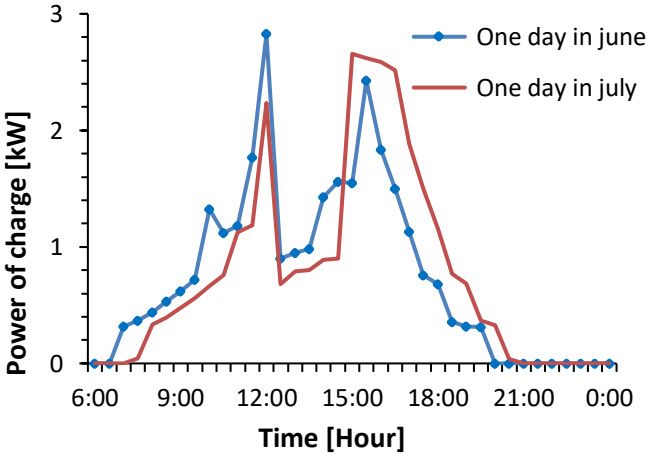

Fig. 12.a. Evolution of the charging time of the storage system.

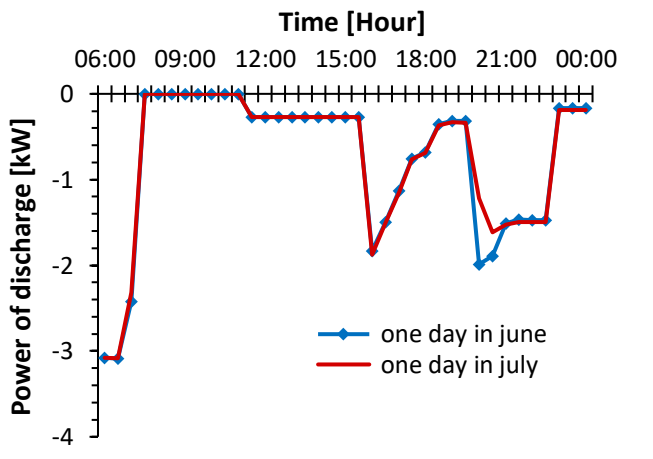

Fig. 12.b. Evolution of the discharging time of the storage system.

In both cases, it appears that charging starts between 7 AM and 8 AM, which corresponds to a low irradiation of 800 Wh/m^2, this positive effect is due mainly to the low consumption that was recorded. With the increase of radiation, the current produced by the generator (current intensity imposed a battery charge), the battery charge rate continues to grow. Although in period of strong sunshine, it appears a load power (load current) decrease, due to the energy excess supplied by the generator before storage.

Figure 13 presents a control and management system of energy. When the battery reaches the maximum state of charge (voltage at maximum threshold), the control system will disconnect the diesel, to avoid electrolysis phenomenon and electrodes corrosion. When the battery voltage reaches its lower threshold value, the battery will reconnected again. This is the principle of maximum voltage regulation.

If the battery is discharged, to avoid electrodessulphation, the control will stop injecting power in the grid from renewable energy and will switch to Diesel, to provide power to the loads. This situation will last until the battery is charged by renewable energy and reaches the level of functioning. The Diesel system will be then stopped. This is called the minimum voltage regulation.

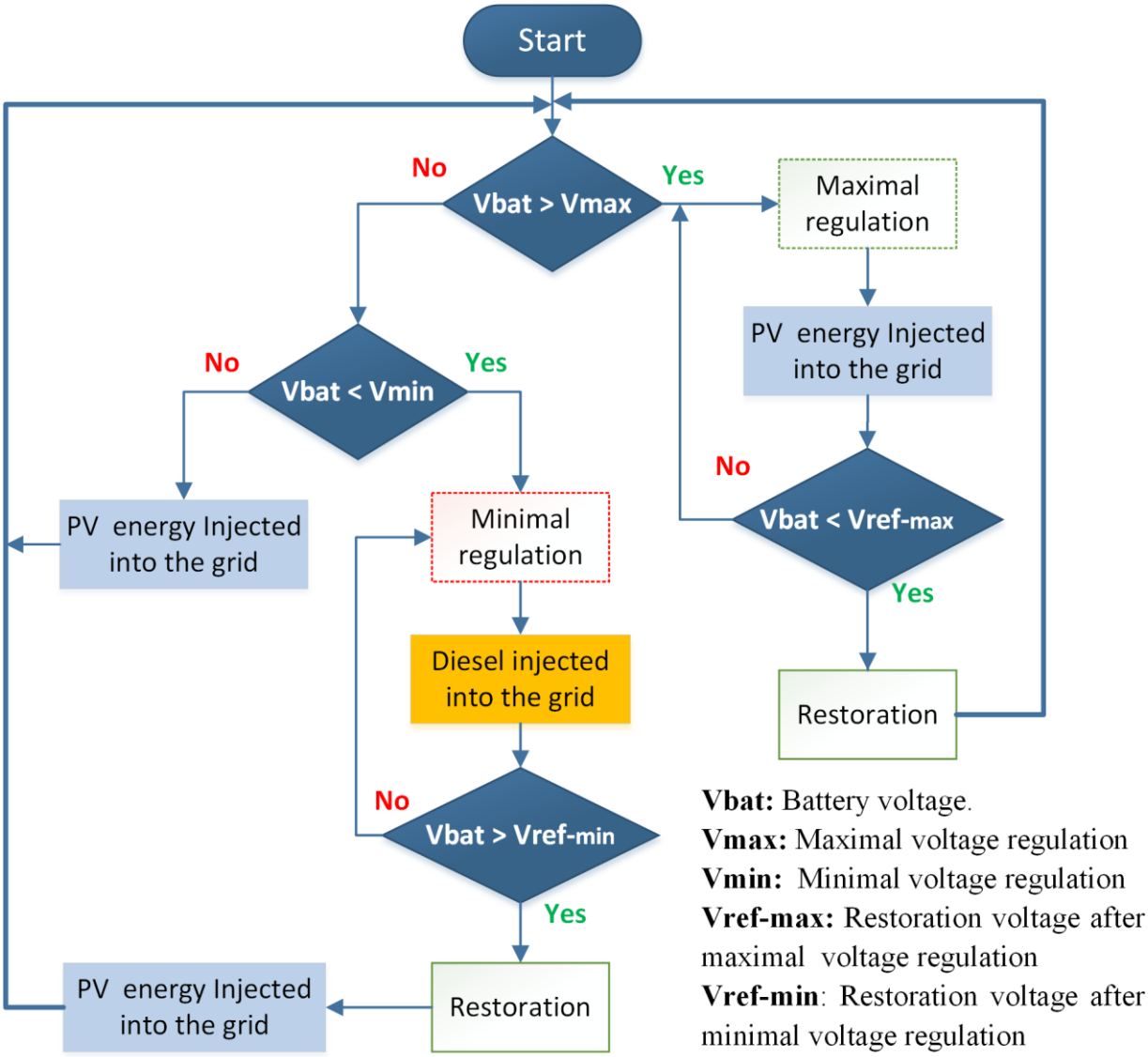

Fig. 13. Flow chart of energy management

After havingstudied, undervariousloads, the behaviorof each elementconstituting the system, theoverall energy balanceof the installation established (Table 6). This assesses theinputs and outputsof the conversion system [39].

Table 6
Global energy balance sheet of PV system.

Days	EG (β)j[Wh/m^2]	E_{pj}[Wh]	E_{schj}[Wh]	$E_{sdischj}$ [Wh]	E_{ecj} [Wh]	E_{scj}[Wh]
July	6528	40358	10950	8833	36322	30874
June	6435	43033	10604	9152	38730	31758

Total system efficiency η_{GS} is equal to the ratio of the consumed energy (output) to received energy on top surface of solar panels.

$$Escj=\eta_G x \eta r x \eta s x \eta c x EG(\beta)j. \textbf{(42)}$$

Thus, the efficiency η_{Gs} is the product of efficiencies of the different PV system components [39].

$$\eta_{GS}=\eta_G x \eta_r x \eta_S x \eta_c \textbf{ (43)}$$

Efficienciesof allsubsystemsand the overallperformanceof the entire systemare shownin the Table 7 bellow:

Table 7
PV system efficiency.

Days	η_G %	ηr %	η_s %	ηc %	η_{GS} %
The 15th of July	10.13	85	81	85	5.93
The 15th of June	11.11	88	86	82	6.90

3.5. Analysis of village charging curve

The analysis of the energy consumption of the village is made through the load curves for a period of one year. Typical and atypical curves recordedduring this period are reviewed and analyzed(Fig. 14.a and 14.b).

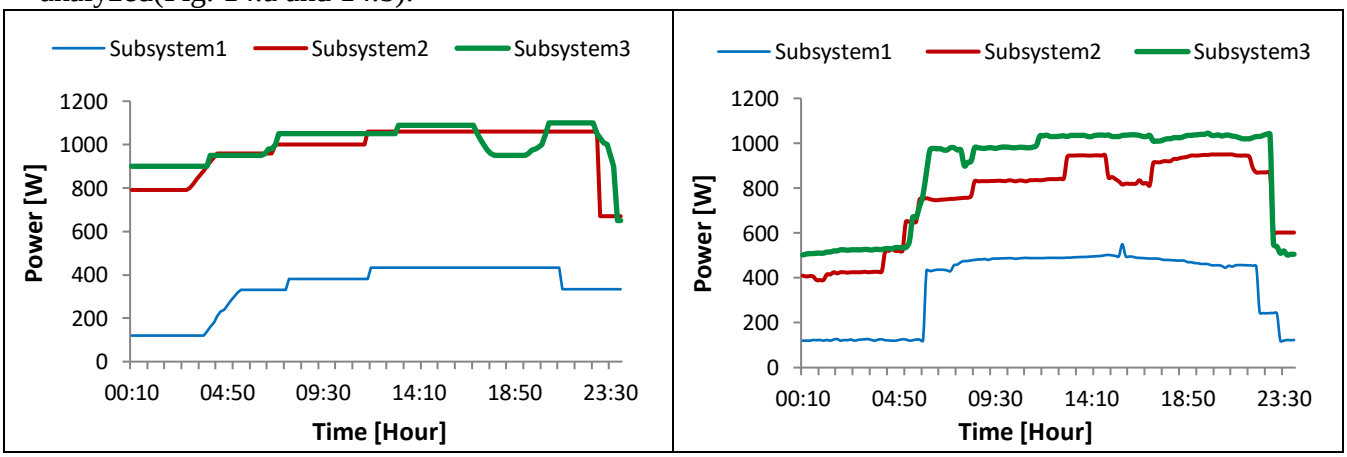

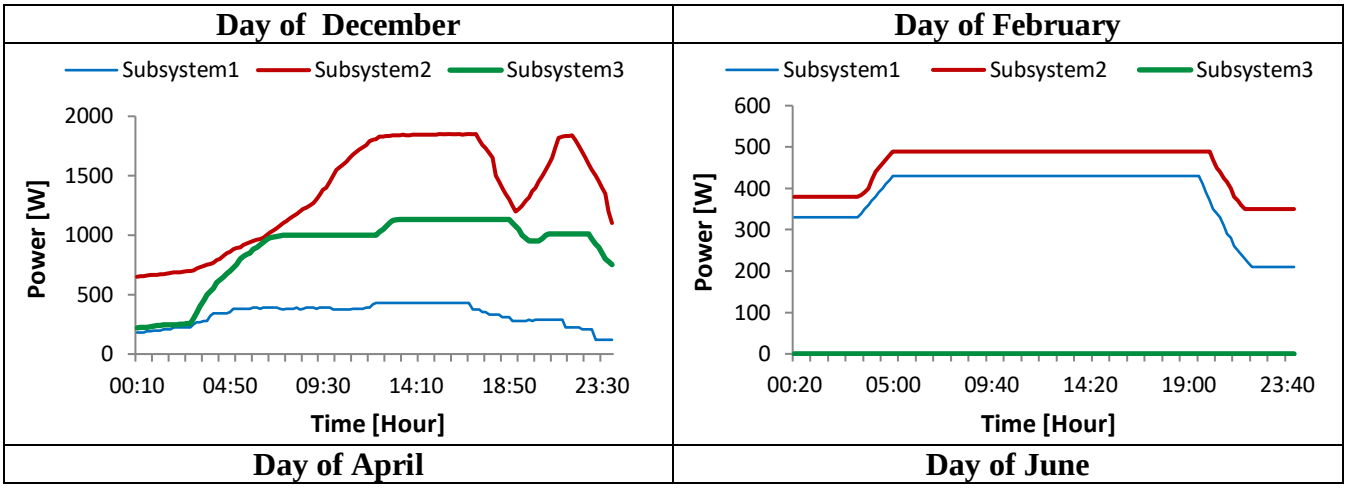

2.

Fig. 14.a. Load curve for the first half of the year.

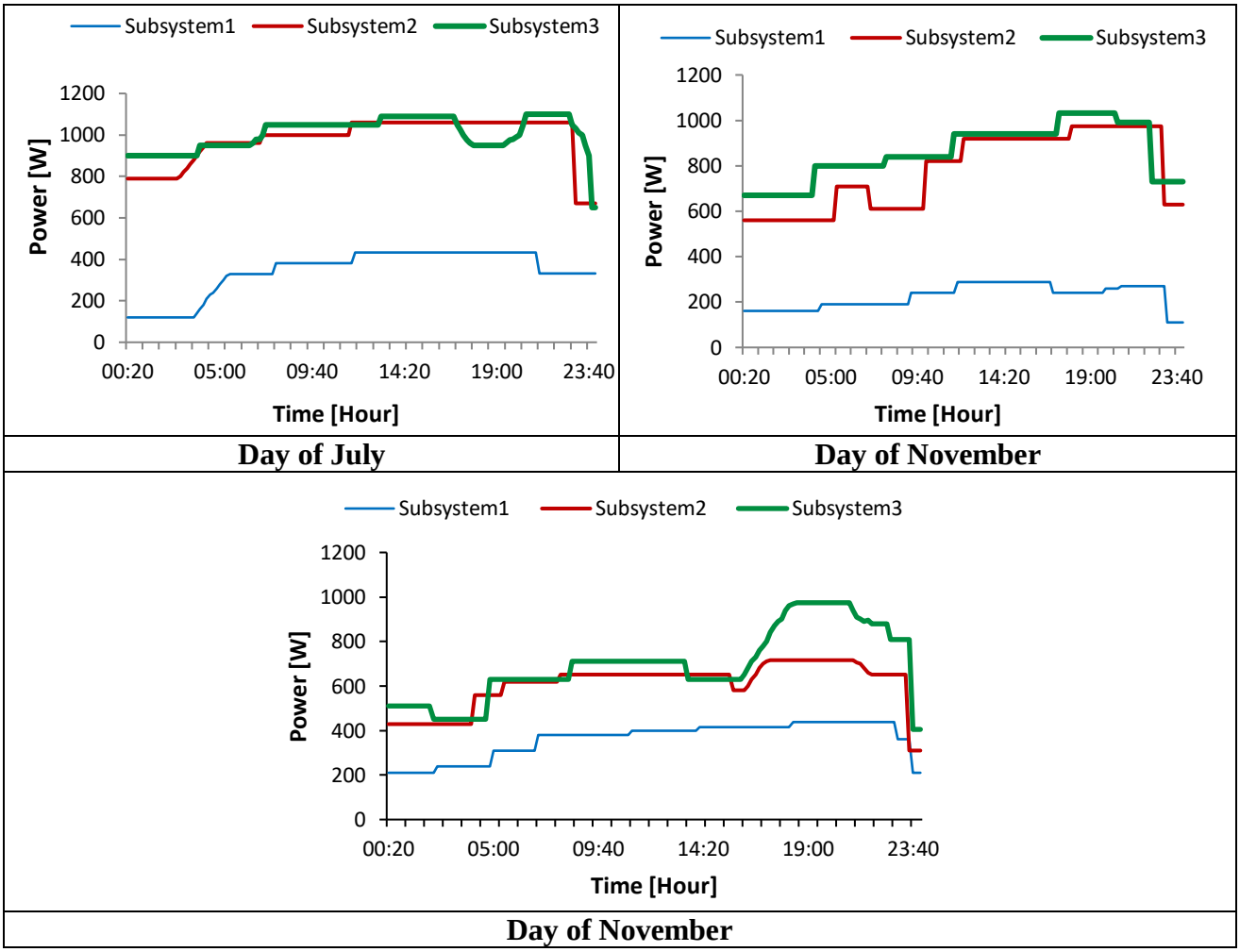

Fig. 14.b. Load curve for the second half of the year.

After analyzing Fig.14.a, and 14.b, it is noticed that:

Days of December and February

The curve recorded the day of December is characterizedbytwo levels. First level at around5 AM,thesecond level from7:50 PM. and then adeclinefrom 11 PM.

It is also found thatthe three subsystems recorda hollowataround 04:30 PM and thena recoveryfrom 6 PMuntilpeaking atabout 9 PM.

Note thatthe ambient temperatureis about 12°Cduring the dayand to2°C at night.

The curve of February is somewhatturbulentcomparedto December especially inthe second subsystem whereit was recordedapower peakat 12 PM,then asudden dropto3 PM,followed bya recoveryto 5 PM,ended with adeclineofaround 11 PM.

Overall, stability in theconsumption pattern, with maintainingthe level of consumptionfor the twosubsystems1 and 3. However,for the subsystem 2, an increase of 17% is recorded in thetime slot6 PM to 11 PM.

The temperature duringthe dayis 15 °C. against6° C at night.

The first informationdelivered bytheload curve is the behaviorof the villagers, it can be detectedthrough itsform as thecurrent drawbecomes more importantfrom 5 AMand 7:50 PMcorresponding towakevillagersto start the dayand returnhome for a maximumuse of electrical appliances and comfort(television. refrigerator).

The load evolution analysisrevealedthatsedentaryBedouinscontinuefor nowthe same behavior,from sunrise at 5 AM(after their prayer) where theirday begins until 12 PMwhena longrespitegenerallyfor a napuntil sunset.

Day of April

For this day, a stability in consumption is seen, with a singularity between 1 PM and 5 PM. The trend is reversed between the subsystems 2 and 3. Indeed, the subsystem 2 has won over the third with an exceptional level of power over respectively 80% and 25% for the subsystems 2 and 3 respectively.

Noting thatforthis month the thermometer displays up to27°C during the day and15°C at night.

The reverse trend in the subsystem 2, which recorded an exceptional current draw due to a wedding ceremony where all the villagers were invited including notable nearby villages. This event explains the increase in power demand increase at both subsystems supplying homes. However, the subsystem powering the school registered a decline in electrical power demand.

Day of June

This isanatypicalcurve patternwithzero consumptionin the thirdsubsystem, a situation which lasted oneweekwithaplausible40% decreaseoftheburden on the secondsubsystemand maintainingthe level of consumptionforthe first subsystem.

This newatypical formis explainedby the fact thatthe subsystem3 fueling tenhouseholdssufferedan electricalincident followedby a tripthe main breaker.

A short circuitproblem at the lampsocketleveling one ofthe villagehomesis the source ofthis disturbance. It took the interventionof one of ourelectricityoperations officerforadjust it (Fig.14.a).

Day of November

For the first considered day, it is found that the subsystems2 and 3 a peak demand shift at 7 PM in comparison with the monthof July takes place until 11 PM (Fig. 14.b)

Temperature during day is about 17°C and 4°C during night.

3.6. Zones competitiveness of photovoltaic solutions and Diesel solution

Assessment and analysis of the competitiveness of the photovoltaic solution compared to the diesel solution, is done through the method developed in section 2.2, knowing that the connection solution from the conventional network, as was reported was in the case study, is technically rejected.

Also, it is necessary to vary the power of the generator, along with the length of the low voltage (L_{BT}) network that feeds this village, to determine the critical distance from which the photovoltaic solution becomes more interesting.

3.6.1. Economic competitiveness

Recalling that the costs of the kWh Photovoltaic and Diesel are given by equations 30 and 32:

$$PV\ cost\ =\ 57.74\ +\ \frac{480}{\mathrm{EG}(\beta,\mathrm{ti})} \quad ; \quad D\ cost = 117.63 + 68058 \times \frac{L_{BT}}{Ec}$$

ΔC = D cost - PV cost;

It is deduced:

$\Delta C > 0 \rightarrow$ photovoltaic is competitive;

$\Delta C < 0 \rightarrow$ diesel is competitive;

$\Delta C = 0 \rightarrow$ limit of competitiveness;

Knowing that $E = \frac{PPV}{KG}$ and $KG = \frac{1}{365 \times K \times \mathrm{EG}(\beta,\mathrm{ti})}$

Thus the graphic representation of $\Delta C = 0$ makes it possible to deduce the economic competitiveness of the two variants:

$\Delta C = 0 \rightarrow PPV = L_{BT} / (1.728 - 0.315 \times EG(\beta,ti))$

In our case, the village is located in an area where solar irradiation EG(β, ti) = 5.4 kWh/m²/day.

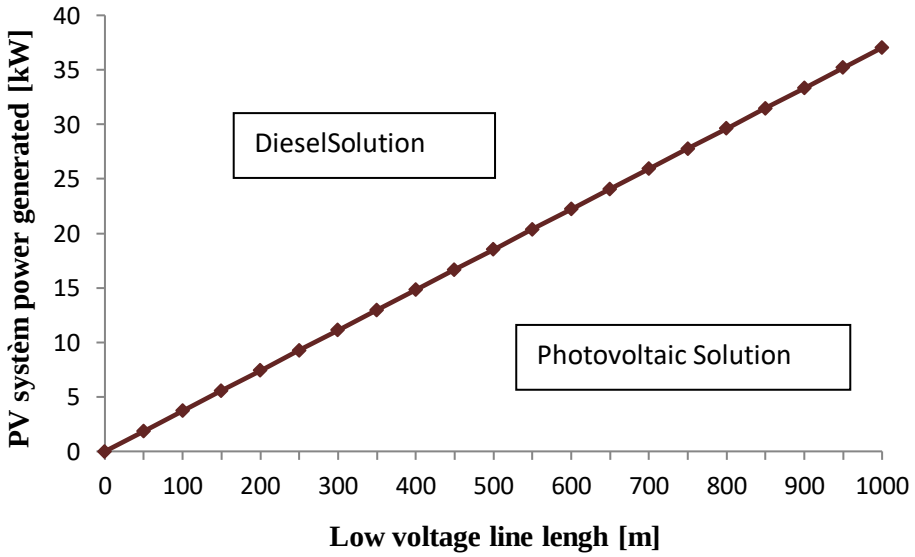

Fig. 15. Competitiveness between photovoltaic and diesel.

The reading of the graphic above Fig.15 shows that up to a critical distance, the connection to the low voltage network (L_{BT}) remains the most competitive. Beyond this distance, it is the photovoltaic solution that is the most interesting.

3.6.2. Competitiveness curve analysis

The interpretation of graph 15, on the competitiveness between diesel and photovoltaic solutions, leads to take the case of two villages, whose power of their generators differs from each other;
One has a peak power of 5.5kW, and the other 10kW.

For the first village:
Up to the critical distance of 150 m length, the connection to the L_{BT} network remains the most advantageous solution, beyond this distance; the photovoltaic solution becomes the most interesting.

For the second village:
Concerning this second customer, the critical distance, from which the photovoltaic solution is more competitive, is 270 m length.
The following Table 8 illustrates what we have just said and gives us critical distances for two types of clients.

Table 8
Critical distance for two types of client.

Customer	Peak power (kWp)	Critical distance (m)
Village 1	5.5	150
Village 2	10.0	270

4. Conclusion

In this research is structured in two main parts. In the first part, an experiment to assess the performance of a system PV under real conditions of exploitation.
In the second part is about comparison between the two solutions of electrification, Diesel engines and photovoltaic systems, using a mathematical approach developed in this research.
The energy characteristics of photovoltaic system were measured with a 30-minute interval measuring station in four seasons. The outcomes of the experiment formed a reliable database, which were used to verify a numerical model developed to predict the energy performance of the module photovoltaic. For the analyzed examples applied to mono crystalline silicon photovoltaic module that feeds Fadnoun village with 736 W/m2, 811 W/m2 and 924 W/m² irradiance and temperature ranging between 35.6°C, 43.3°C and 46.8 °C, the errors are small. The model fits with great accuracy the I-V characteristic and converges in all studied cases. However, it requires good measures in adjacent areas with ISC, Voc, Im and Vm and measuring slopes in ISC and in Voc.
Thanks to this works, an over sizing of the PV system was detected can be claimed that an extension of the village by more than 40%.
The second part of this study revealed that up to a critical distance, the connection to the low voltage network (L_{BT}) remains the most competitive. Beyond this distance, it is the photovoltaic solution that is the most appropriate option. In addition, the reliability and the villagers' lifestyle

influences the energy consumption can contribute to significant increase in the annual electricity generation of the PV system.

Finally, the outcomes of this study can be used as benchmark to analysis the photovoltaic systems and to predict the opportunity to embark on a photovoltaic or other installation in order to control similar investments in the future.

References

1. Activity report and consolidated revenue and expenditure account **Sonelgaz group**. 2015.
2. J.C. Borel,Supporting study of the definition of climatic zones in Algeria. Ch C.S.T.B. (1962) 456. paris.
3. A. Hadj Arab, B. Ait Driss,M. Amimeur, F. Lorenzo,. Photovoltaic system sizing forAlgéria.**Solar Energy,** 54(1995) 99-104.
4. K. Abdeladim, A. Razagui, S. Semaoui, and A. Hadj Arab, Updating Algerian solar atlas using MEERA-2 data source. **Energy Reports**, 6 (2020) 281-287.
5. B. Bouzidi, . Analysis of the feasibility and economic efficiency of photovoltaic. solar energy, (2004) water pumping systems. **Master thesis ENP**.
6. EM. Nfah, and JM. Ngundam, Modelling of wind/diesel/battery hybrid power systems for far North Cameroon. **Energy Conversion Management,** 9 (2004) 1295–301.
7. M. Ansong, L.D.Mensaha, and S.M. Adaramola,Techno-economic analysis of a hybrid system to power a mine in an off-grid area in Ghana.**Sustainable Energy Technologies and Assessments**, 23 (2017) 48-56.
8. M. Bortolini, M. Gamberi, A. Graziani, F. Pilati, Economic and environmental bi-objective design of an off- grid photovoltaic–battery–diesel generator hybrid. **EnergyConversionManagement,** 06(2015) 1024–1038.
9. MS Ismail, M Moghavvemi, and TMI Mahlia,. Techno-economic analysis of an optimized photovoltaic and diesel generator hybrid power system for remote houses in a tropical climate. **Energy Conversion Management,** 69 (2013)163–73.
10. MS Ismail, M Moghavvemi, and TMI Mahlia, Design of an optimized photovoltaic and microturbine hybrid power system for a remote small community: Case study of Palestine. **Energy Conversion Management,** 73 (2013) 57–68.
11. US. Kumar, and PS. Manoharan, Economic analysis of hybrid power systems (PV/diesel) in different climatic zones of Tamil Nadu. **Energy Conversion Management,** 80 (2014) 469 -476.
12. M. Shahrestani,R. Yao,E. Essah,L. Shao,A. Oliveira,A. Hepbasli,E. Biyik,T. del Caño,E. Rico, and JL. Lechón,Experimental and numerical studies to assess the energyperformance of naturally ventilated PV façade systems.**Solar Energy,** 147 (2017) 37-51.
13. G. Djoudi, A. Hadj Arab, and H. Salhi, Improvement and validation of PV motor-pump model for PV pumping system performance analysis. **Solar Energy,**142 (2017) 310-320.
14. Y. Kabalci, E. Kabalci, R. Canbaz, and A. Calpbinici, Design and implementation of a solar plant and irrigation system with remote monitoring and remote control infrastructures. **Solar Energy,** 139 (2016) 506-517.
15. D.P. Astudillo, and D. Bachour,Variability of measured Global Horizontal Irradiation throughout Qatar.**Solar Energy,** 119 (2015) 169-178.
16. R Tapakis,S Michaelides, and A.G Charalambides,Computations of diffuse fraction of global irradiance, Part 1 – Analytical modelling. **Solar Energy,** 139 (2016) 711-722.
17. M. Iqbal, An introduction to solar irradiation. Academic Press. Toronto. (1983) 390.

18. E. Lorenzo, Electricidad solar. Ingenieria de los sistemas fotovoltaicos. **Progensa. Sevilla**.(1994) 338.
19. F. Frutos, V. Ruiz, and J. Gutirrez,Correlation between the solar diffuse and global radiation for Madrid. **Internation ale Review of Heliotechnics**, (1985)7-12p.
20. P Upadhyay,S Pulipaka,M Sharma, and R Kumar,A proposed maximum power point operating strategy for photovoltaic applications using monthly irradiance estimates. **Solar Energy,** 141(2017) 266-277.
21. J.E. Hay, and D.C. McKay, Estimating solar irradiance on inclined surfaces a review and assessment of methodologies. **Solar. Energy,** 3 (1985) 203-240.
22. D. Soto, W. Klein, S.A, and W.A, Beckam, Improvement and validation of a model for photovoltaic array. 7 (2006) 8-88.
23. A. Hadj Arab, F. Chenlo, K. Mukadam and J.L.Balenzategui, Performance of PV water pumping system.**renewable Energy,** 18(1999) 191-204.
24. A. Dolora, S. Leva, G. Manzolini, Comparison of different physical models for PV power output prediction. **Solar Energy,** 119 (2015) 83-99.
25. A. Hadj Arab,., F. Chenlo, M.Benghanem, Loss-Load probability of photovoltaic water pumping system. **Solar Energy,** 76 (2004) 713-723.
26. T. Fogelman, and Montiloin, Photovoltaic installation in isolated habitat. C-Y. Chaudoreille- Edisaud. Aix-en-Provence(1983).
27. A Yahiaoui,K Benmansour,and M Tadjine,Control, analysis and optimization of hybrid PV- Diesel-Battery systems for isolated rural city in Algeria. **Solar Energy,** 137 (2016) 1-10.
28. Course technical-economic study of solar electrification solutions.**ETB Sonelgaz** (2010).
29. Renewable Power Génération Costs in 2014.(**The International Renewable Energy Agency) IRENA**, January 2015.
30. District Directorate of tourism Illizi, TASSILI N'AJJER, through tourism. "We discover the other but above all oneself is discovered "(2013).
31. J Tanesab,., D Parlevliet,., J.Whale, , T Urmee,., and T Pryor,.,. The contribution of dust to performance degradation of PV modules in a temperate climate zone. **Solar Energy,** 120(2015) 147-157.
32. W. Javed, Y. Wubulikasimu, B. Figgis, and B. Guo, Characterization of dust accumulated on photovoltaic panels in Doha, Qatar. **Solar Energy,** 142 (2017) 1-340.
33. M. Husam, A. Walwil, A.Mukhaimer, F.A., Al-Sulaiman, and A.M. Syed Said,. Comparativestudies of encapsulation and glass surface modification impacts on PV performance in adesert climate. **Solar Energy,** 142 (2017) 288-298.
34. A. Hussein, T. Kazem, T. MiqdamChaichanc, Ali H.A. Al-Waelib, and K.Sopian, A novel model and experimental validation of dust impact on grid-connected photovoltaic system performance in Northern Oman.**Solar Energy**, 206 (2020) 564-578.
35. CX2000-4-CLK AMC, Direct feed three phase meter, Instructions manual (2010).
36. F Sick, and T Erge, Photovoltaics in buildings, a design handbook for architects and engineers. **International Energy AgencyXYZ PublishingCompany,** Paris. France(2010).
37. J. Sunab, L. Zhengrong, F. Xiao, and J. Xiao, Generation of typical meteorological year for integrated climate based daylight modeling and building energy simulation. **Renewable Energy**, 160 (2020) 721-729.
38. A.K. Shukla, K. Sudhakar, and P. Baredar, Design, simulation and economic analysis of standalone roof top solar PV system in India. **Solar Energy,** 136 (2016) 437-449.
39. R.C. Neville, **solar energy conversion**. The solar cell. Elsevier (1978).